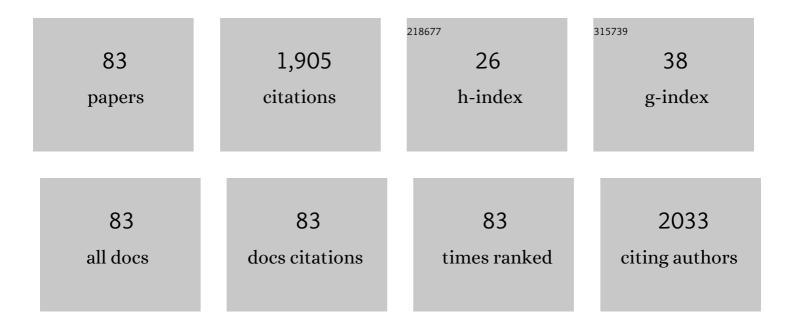
Richard G Spencer

List of Publications by Year in descending order

Source: https://exaly.com/author-pdf/1005821/publications.pdf Version: 2024-02-01



#	Article	IF	CITATIONS
1	Insights into human cerebral white matter maturation and degeneration across the adult lifespan. NeuroImage, 2022, 247, 118727.	4.2	30
2	Differential associations between apolipoprotein E alleles and cerebral myelin content in normative aging. NeuroImage, 2022, 251, 118988.	4.2	9
3	Stabilization of parameter estimates from multiexponential decay through extension into higher dimensions. Scientific Reports, 2022, 12, 5773.	3.3	5
4	Input layer regularization for magnetic resonance relaxometry biexponential parameter estimation. Magnetic Resonance in Chemistry, 2022, 60, 1076-1086.	1.9	0
5	Evidence of association between obesity and lower cerebral myelin content in cognitively unimpaired adults. International Journal of Obesity, 2021, 45, 850-859.	3.4	19
6	Sex and age-related differences in cerebral blood flow investigated using pseudo-continuous arterial spin labeling magnetic resonance imaging. Aging, 2021, 13, 4911-4925.	3.1	30
7	Ageâ€related estimates of aggregate <i>g</i> â€ratio of white matter structures assessed using quantitative magnetic resonance neuroimaging. Human Brain Mapping, 2021, 42, 2362-2373.	3.6	19
8	Reply to Roemer and Guermazi: Early biochemical changes on MRI can predict risk of symptomatic progression. Proceedings of the National Academy of Sciences of the United States of America, 2021, 118, e2024679118.	7.1	0
9	Parsimonious modeling of skeletal muscle perfusion: Connecting the stretched exponential and fractional Fickian diffusion. Magnetic Resonance in Medicine, 2021, 86, 1045-1057.	3.0	6
10	Association of central arterial stiffness with hippocampal blood flow and N-acetyl aspartate concentration in hypertensive adult Dahl salt sensitive rats. Journal of Hypertension, 2021, 39, 2113-2121.	0.5	1
11	Maturation and degeneration of the human brainstem across the adult lifespan. Aging, 2021, 13, 14862-14891.	3.1	11
12	Investigation of the association between cerebral iron content and myelin content in normative aging using quantitative magnetic resonance neuroimaging. NeuroImage, 2021, 239, 118267.	4.2	34
13	Adult brain aging investigated using BMC-mcDESPOT–based myelin water fraction imaging. Neurobiology of Aging, 2020, 85, 131-139.	3.1	41
14	Quantitative age-dependent differences in human brainstem myelination assessed using high-resolution magnetic resonance mapping. NeuroImage, 2020, 206, 116307.	4.2	20
15	Four-angle method for practical ultra-high-resolution magnetic resonance mapping of brain longitudinal relaxation time and apparent proton density. Magnetic Resonance Imaging, 2020, 66, 57-68.	1.8	0
16	Special issue on inverse problems in biomedical magnetic resonance. NMR in Biomedicine, 2020, 33, e4417.	2.8	1
17	Parsimonious discretization for characterizing multiâ€exponential decay in magnetic resonance. NMR in Biomedicine, 2020, 33, e4366.	2.8	5
18	Association of cerebral blood flow with myelin content in cognitively unimpaired adults. BMJ Neurology Open, 2020, 2, e000053.	1.6	23

#	Article	IF	CITATIONS
19	Nonlinear associations of neurite density and myelin content with age revealed using multicomponent diffusion and relaxometry magnetic resonance imaging. NeuroImage, 2020, 223, 117369.	4.2	25
20	Enabling early detection of osteoarthritis from presymptomatic cartilage texture maps via transport-based learning. Proceedings of the National Academy of Sciences of the United States of America, 2020, 117, 24709-24719.	7.1	29
21	Impact of pulse sequence, analysis method, and signal to noise ratio on the accuracy of intervertebral disc T 2 measurement. JOR Spine, 2020, 3, e1102.	3.2	3
22	A Tutorial Introduction to Inverse Problems in Magnetic Resonance. NMR in Biomedicine, 2020, 33, e4315.	2.8	7
23	\$N\$-Dimensional Tensor Completion for Nuclear Magnetic Resonance Relaxometry. SIAM Journal on Imaging Sciences, 2020, 13, 176-213.	2.2	2
24	A simple and fast adaptive nonlocal multispectral filtering algorithm for efficient noise reduction in magnetic resonance imaging. Magnetic Resonance Imaging, 2019, 55, 133-139.	1.8	6
25	Stabilization of T ₂ relaxation and magnetization transfer in cartilage explants by immersion in perfluorocarbon liquid. Magnetic Resonance in Medicine, 2019, 81, 3209-3217.	3.0	3
26	The Role of Muscle Perfusion in the Age-Associated Decline of Mitochondrial Function in Healthy Individuals. Frontiers in Physiology, 2019, 10, 427.	2.8	31
27	Steadyâ€ s tate doubleâ€angle method for rapid <i>B</i> ₁ mapping. Magnetic Resonance in Medicine, 2019, 82, 189-201.	3.0	12
28	Diffusionâ€weighted MRI with intravoxel incoherent motion modeling for assessment of muscle perfusion in the thigh during postâ€exercise hyperemia in younger and older adults. NMR in Biomedicine, 2019, 32, e4072.	2.8	17
29	Evidence of demyelination in mild cognitive impairment and dementia using a direct and specific magnetic resonance imaging measure of myelin content. Alzheimer's and Dementia, 2018, 14, 998-1004.	0.8	105
30	Fisher information and Cramérâ€Rao lower bound for experimental design in parallel imaging. Magnetic Resonance in Medicine, 2018, 79, 3249-3255.	3.0	15
31	Rapid B1 field mapping at 3â€⊤ using the 180° signal null method with extended flip angle. Magnetic Resonance Imaging, 2018, 53, 173-179.	1.8	6
32	Use of the NESMA Filter to Improve Myelin Water Fraction Mapping with Brain MRI. Journal of Neuroimaging, 2018, 28, 640-649.	2.0	19
33	Spatially adaptive unsupervised multispectral nonlocal filtering for improved cerebral blood flow mapping using arterial spin labeling magnetic resonance imaging. Journal of Neuroscience Methods, 2018, 309, 121-131.	2.5	12
34	Predicting early symptomatic osteoarthritis in the human knee using machine learning classification of magnetic resonance images from the osteoarthritis initiative. Journal of Orthopaedic Research, 2017, 35, 2243-2250.	2.3	70
35	Clinical high-resolution mapping of the proteoglycan-bound water fraction in articular cartilage of the human knee joint. Magnetic Resonance Imaging, 2017, 43, 1-5.	1.8	7
36	The effect of noise and lipid signals on determination of Gaussian and nonâ€Gaussian diffusion parameters in skeletal muscle. NMR in Biomedicine, 2017, 30, e3718.	2.8	15

#	Article	IF	CITATIONS
37	Point Estimates of Test Sensitivity and Specificity from Sample Means and Variances. American Statistician, 2017, 71, 81-87.	1.6	1
38	Noise Estimation and Reduction in Magnetic Resonance Imaging Using a New Multispectral Nonlocal Maximum-likelihood Filter. IEEE Transactions on Medical Imaging, 2017, 36, 181-193.	8.9	29
39	Rapid simultaneous high-resolution mapping of myelin water fraction and relaxation times in human brain using BMC-mcDESPOT. NeuroImage, 2017, 147, 800-811.	4.2	52
40	L ₁ , L _{<i>p</i>} , L ₂ , and elastic net penalties for regularization of Gaussian component distributions in magnetic resonance relaxometry. Concepts in Magnetic Resonance Part A: Bridging Education and Research, 2017, 46A, .	0.5	11
41	Multiparametric Classification of Skin from Osteogenesis Imperfecta Patients and Controls by Quantitative Magnetic Resonance Microimaging. PLoS ONE, 2016, 11, e0157891.	2.5	4
42	Analysis of mcDESPOT―and CPMGâ€derived parameter estimates for two omponent nonexchanging systems. Magnetic Resonance in Medicine, 2016, 75, 2406-2420.	3.0	40
43	Anomalous T ₂ relaxation in normal and degraded cartilage. Magnetic Resonance in Medicine, 2016, 76, 953-962.	3.0	29
44	Cytochrome b5 reductase and the control of lipid metabolism and healthspan. Npj Aging and Mechanisms of Disease, 2016, 2, 16006.	4.5	57
45	Improved determination of the myelin water fraction in human brain using magnetic resonance imaging through Bayesian analysis of mcDESPOT. NeuroImage, 2016, 127, 456-471.	4.2	50
46	2D sparse sampling algorithm for ND Fredholm equations with applications to NMR relaxometry. , 2015, , .		4
47	Sensitivity and specificity of univariate MRI analysis of experimentally degraded cartilage under clinical imaging conditions. Journal of Magnetic Resonance Imaging, 2015, 42, 136-144.	3.4	8
48	Incorporation of nonzero echo times in the SPGR and bSSFP signal models used in mcDESPOT. Magnetic Resonance in Medicine, 2015, 74, 1227-1235.	3.0	35
49	Incorporation of rician noise in the analysis of biexponential transverse relaxation in cartilage using a multiple gradient echo sequence at 3 and 7 tesla. Magnetic Resonance in Medicine, 2015, 73, 352-366.	3.0	37
50	Bayesian analysis of transverse signal decay with application to human brain. Magnetic Resonance in Medicine, 2015, 74, 785-802.	3.0	16
51	Classification of histologically scored human knee osteochondral plugs by quantitative analysis of magnetic resonance images at 3T. Journal of Orthopaedic Research, 2015, 33, 640-650.	2.3	13
52	Articular Cartilage of the Human Knee Joint: In Vivo Multicomponent T2 Analysis at 3.0 T. Radiology, 2015, 277, 477-488.	7.3	28
53	Prediction of cartilage compressive modulus using multiexponential analysis of <i>T</i> ₂ relaxation data and support vector regression. NMR in Biomedicine, 2014, 27, 468-477.	2.8	4
54	Metabolic abnormalities and hypoleptinemia in α-synuclein A53T mutant mice. Neurobiology of Aging, 2014. 35. 1153-1161.	3.1	23

#	Article	IF	CITATIONS
55	How Do Statistical Differences in Matrix-sensitive Magnetic Resonance Outcomes Translate Into Clinical Assignment Rules?. Journal of the American Academy of Orthopaedic Surgeons, The, 2013, 21, 438-439.	2.5	9
56	Near Infrared Spectroscopy as a Method for Non-Destructive Monitoring of Engineered Cartilage Growth. , 2013, , .		2
57	CHAPTER 14. Applications of MRI and MRS in Cartilage Therapeutics and Tissue Engineering. New Developments in NMR, 2013, , 376-404.	0.1	1
58	Stabilization of the inverse Laplace transform of multiexponential decay through introduction of a second dimension. Journal of Magnetic Resonance, 2013, 236, 134-139.	2.1	33
59	Assessment of Changes in Engineered Cartilage Using Infrared Spectroscopy and Mechanical Analysis. , 2013, , .		Ο
60	How Do Statistical Differences in Matrix-sensitive Magnetic Resonance Outcomes Translate Into Clinical Assignment Rules?. Journal of the American Academy of Orthopaedic Surgeons, The, 2013, 21, 438-439.	2.5	6
61	Characterization of Engineered Cartilage Constructs Using Multiexponential <i>T</i> ₂ Relaxation Analysis and Support Vector Regression. Tissue Engineering - Part C: Methods, 2012, 18, 433-443.	2.1	15
62	Multivariate analysis of cartilage degradation using the support vector machine algorithm. Magnetic Resonance in Medicine, 2012, 67, 1815-1826.	3.0	31
63	Improved MRâ€based characterization of engineered cartilage using multiexponential <i>T</i> ₂ relaxation and multivariate analysis. NMR in Biomedicine, 2012, 25, 476-488.	2.8	28
64	Magnetic resonance in tissue engineering. NMR in Biomedicine, 2012, 25, 401-401.	2.8	1
65	Mapping proteoglycanâ€bound water in cartilage: Improved specificity of matrix assessment using multiexponential transverse relaxation analysis. Magnetic Resonance in Medicine, 2011, 65, 377-384.	3.0	44
66	Improved specificity of cartilage matrix evaluation using multiexponential transverse relaxation analysis applied to pathomimetically degraded cartilage. NMR in Biomedicine, 2011, 24, 1286-1294.	2.8	30
67	Effects of frozen storage and sample temperature on water compartmentation and multiexponential transverse relaxation in cartilage. Magnetic Resonance Imaging, 2011, 29, 561-567.	1.8	16
68	Anomalous NMR relaxation in cartilage matrix components and native cartilage: Fractional-order models. Journal of Magnetic Resonance, 2011, 210, 184-191.	2.1	43
69	Magnetic Resonance Studies of Macromolecular Content in Engineered Cartilage Treated with Pulsed Low-Intensity Ultrasound. Tissue Engineering - Part A, 2011, 17, 407-415.	3.1	15
70	Characterization of <i>Ex Vivo</i> –Generated Bovine and Human Cartilage by Immunohistochemical, Biochemical, and Magnetic Resonance Imaging Analyses. Tissue Engineering - Part A, 2010, 16, 2183-2196.	3.1	18
71	Nondestructive Assessment of Engineered Cartilage Constructs Using Near-Infrared Spectroscopy. Applied Spectroscopy, 2010, 64, 1160-1166.	2.2	61
72	Multicomponent T ₂ relaxation analysis in cartilage. Magnetic Resonance in Medicine, 2009, 61, 803-809.	3.0	149

#	Article	IF	CITATIONS
73	Sensitivity and specificity of univariate MRI analysis of experimentally degraded cartilage. Magnetic Resonance in Medicine, 2009, 62, 1311-1318.	3.0	31
74	Classification of degraded cartilage through multiparametric MRI analysis. Journal of Magnetic Resonance, 2009, 201, 61-71.	2.1	46
75	Assessment of tissue repair in full thickness chondral defects in the rabbit using magnetic resonance imaging transverse relaxation measurements. Journal of Biomedical Materials Research - Part B Applied Biomaterials, 2008, 86B, 375-380.	3.4	21
76	Noninvasive Assessment of Glycosaminoglycan Production in Injectable Tissue-Engineered Cartilage Constructs Using Magnetic Resonance Imaging. Tissue Engineering - Part C: Methods, 2008, 14, 243-249.	2.1	25
77	Gender Differences in Musculoskeletal Lipid Metabolism as Assessed by Localized Two-Dimensional Correlation Spectroscopy. Magnetic Resonance Insights, 2008, 2008, 1-6.	2.5	8
78	Measurement of spin-lattice relaxation times and chemical exchange rates in multiple-site systems using progressive saturation. Magnetic Resonance in Medicine, 2007, 58, 8-18.	3.0	5
79	Effects of formalin fixation and collagen cross-linking onT2 and magnetization transfer in bovine nasal cartilage. Magnetic Resonance in Medicine, 2007, 57, 1000-1011.	3.0	65
80	Fourier transform infrared imaging and MR microscopy studies detect compositional and structural changes in cartilage in a rabbit model of osteoarthritis. Analytical and Bioanalytical Chemistry, 2007, 387, 1601-1612.	3.7	69
81	Development of cardiomyopathy in response to chronic βâ€adrenegric stimulation of transgenic mouse overexpressing the exonâ€22 isoform of the human Ca _v 1.2 channel _{α1C} subunit as revealed by magnetic resonance imaging. FASEB Journal, 2007, 21, A583.	0.5	0
82	Compatibility of Gd-DTPA perfusion and histologic studies of the brain. Magnetic Resonance Imaging, 2006, 24, 27-31.	1.8	14
83	An analysis of the integration between articular cartilage and nondegradable hydrogel using magnetic resonance imaging. Journal of Biomedical Materials Research - Part B Applied Biomaterials, 2006, 778, 144-148	3.4	40